Proceedings of OMAE 2017
36th International Conference on Ocean, Offshore and Arctic Engineering
June 25-30, 2017, Trondheim, Norway

OMAE2017-62489

STATIC STABILITY OF FLOATING UNITS IN OPERATIONAL CONDITIONS: A PHYSICS-DRIVEN APPROACH

Neil Luxcey *
SINTEF Ocean AS †
Norwegian Marine Technology Research Institute
POB 4125 Valentinlyst NO-7450 Trondheim
Norway
neil.luxcey@sintef.no*

Øystein Johannessen
STATOIL ASA
Strandvegen 4
NO-7500 Stjørdal
Norway

Sébastien Fouques
SINTEF Ocean AS
Norwegian Marine Technology Research Institute
POB 4125 Valentinlyst NO-7450 Trondheim
Norway

ABSTRACT

When designing a new floating unit concept, static stability computations are performed in order to check stability criteria defined in regulations. Calculations for design conditions generally include the estimation of buoyancy force, gravity force and wind force acting on the floater for a given condition and a desired axis of rotation. However, when studying the stability of a floating platform in operational conditions, all external forces acting on the unit should be comprised in the assessment in order to get a more realistic - and even physically admissible - picture of the platform stability. Those forces include among others wind, current and anchor line system forces. In addition, limiting the study to one axis of rotation may not provide a complete picture of the floater stability, especially when the hull is of a semi-submersible type.

Following this physical approach, a numerical tool has been developed based on the SINTEF Ocean's SIMA software package. The latter package initially includes a time domain simulator of complex multibody systems for marine operations. The developed tool provides accurate physical models for each force component that may have effects on the stability. It opens the possibility to study the operational stability of a floater without restraining the study to one axis of rotation. It also allows the analysis of damaged conditions with large inclination angles.

This paper describes the model implemented in this numerical tool. Validation work is presented for simple geometries. Results from an operational stability study of a semi-submersible are discussed. Finally, possible further work is discussed.

INTRODUCTION

Static stability computation is a central part of the design procedure of all floating units. It includes dimensioning the geometry and the mass distribution of the structure so that its inclination angle remains within an acceptable range in various environmental conditions. Acceptance criteria can be found in different standards and regulations, e.g. DNV-GL [1] and IMO [2] respectively. The main loads to be included in the calculation are the forces and moments due to gravity, buoyancy and wind, as well as other physical effects that may be of importance: current, thrusters and ice loads. In the ship industry, dedicated software are used for that purpose.

The static stability is often analyzed by considering a one-dimensional problem, where the rotation of the floating unit about a given axis and the corresponding restoring moment about this axis are studied. This is a practical approach for floating units for which it is easy to identify one axis with low stiffness. This is typically the case for ship-shaped structures; the roll axis is much weaker than the pitch axis in the sense that the latter generally benefits from a larger hydrostatic stiffness.

*Address all correspondence to this author.
†Earlier MARINTEK, SINTEF Ocean from 1st January 2017 through a merger internally in the SINTEF Group

Thus, in such cases, studying the restoring moment about one rotation axis only is relevant. However, when considering floating structures of semi-submersible type, the situation is different. Weak axes and strong axes are not necessarily easy to identify, and two perpendicular axes might be of the same strength. This entails a possible strong coupling between the degrees of freedom, meaning that e.g. a rotation in roll might cause a strong moment in pitch. In such cases, restraining the stability study to the study of one axis at a time is not practical and may lead to a wrong picture of the floater stability. Although various methods can be found in the literature (see e.g. [3] and [4]), rules and regulations bodies do not provide a definite calculation method to identify critical axes for a semi-submersible. Thus, there is a need for flexible numerical tools that include possibilities to study static stability of floaters in a multidimensional space.

When studying anchored floating units, static stability calculations are often performed assuming that the unit is freely floating, as specified in the rules and regulations as e.g. in [2], section 3.2.6. The forces and moments from the mooring lines are ignored if small, or modeled as constant deadweight if significant. In some cases, they might be represented as a linear stiffness matrix. However, none of those solutions captures correctly the physics of the mooring lines for large offsets of the unit in the horizontal plane (due to e.g. large current velocity), or large inclination angles (due to e.g. a damaged condition). In addition, loads due to mooring line tension may have important consequences on the unit equilibrium in some situations; a too simplified mooring line model may actually lead to wrong conclusions regarding the stability of the unit. The effect of modeling the anchor lines using a catenary model has been studied in e.g. [5]. Therefore, novel numerical tools should include the possibility to model the mooring lines in a realistic way.

During the past 30 years, advances in modelling the response of offshore structures have been substantial, and in the meantime, computational power has increased considerably. Thus, the need for simplifications should not be considered as the main driving factor when it comes to physical modelling. The approach presented in this paper is then to start from the correct modelling of the physics, in order to obtain stability calculation results as realistic as possible (see discussions in e.g. [4]). For that purpose, the SIMA software package is used as a starting point, since it already provides a considerable amount of physics modelling possibilities. Then additional physical models and tools specific to stability computations are implemented and added to SIMA. A method similar to the one described in [3] is used to study the floater's stability in multidimensional space: total moments, i.e. including all the external forces, are computed as functions of fixed trim and heel. Ultimately, the goal of the presented approach is to obtain a generalized tool that aims at assessing floater stability.

This paper presents the current state of the developed tool, and focuses on the importance of realistic physical modelling. One should note that the full assessment of stability criteria as well as systematic assessment of the mooring lines modelling are not covered.

This paper first describes the description of the implemented numerical models, before validation of hydrostatic computation by means of simple geometries is documented. Real case studies are then presented to illustrate the potential of the developed tool. Finally, possible further work is discussed.

DESCRIPTION OF NUMERICAL MODEL

In order to answer the needs described in the previous section, a static calculation tool was developed and included in the SIMO program (SImulation of Marine Operations) [6], which is part of the SINTEF Ocean's software suite SIMA. SIMO is a time domain simulation program to study the motion and station keeping of multibody systems. Numerical models of various forces, such as anchor line forces, are available. The goal being to assess accurately the static stability of floating units, numerical models of the following forces have been developed and made available in SIMO:

- hydrostatic pressure on the floater hull
- weight of fluid in ballast tanks
- wind and current forces on the floater hull

The implemented numerical models corresponding to those forces are described in the following, as well as the different types of calculation methods.

Notations

We consider a body in calm water. Bold notation represents vectors and matrices. In addition, we use the following notations:

- $\{\mathrm{n}\} = (O, \boldsymbol{n_1}, \boldsymbol{n_2}, \boldsymbol{n_3})$ is an Earth-fixed coordinate system with origin O, $\boldsymbol{n_3}$ pointing upwards.
- $\{\mathrm{b}\} = (O_b, \boldsymbol{b_1}, \boldsymbol{b_2}, \boldsymbol{b_3})$ is a coordinate system fixed to the floating structure, with origin O_b. Surge, sway and heave motions are translational motions of the floating structure along the axes $\boldsymbol{b_1}$, $\boldsymbol{b_2}$ and $\boldsymbol{b_3}$, respectively.
- $\boldsymbol{r}_n = (x_b, y_b, z_b)^T$ is the position of the body origin O_b in $\{n\}$
- $\boldsymbol{\Theta}_n = (\phi, \theta, \psi)^T$ are the Euler angles describing the attitude of the body $\{b\}$ in $\{n\}$, as defined in Fig.1

- $\{b_o\}$=($O_{bo}, \boldsymbol{b_{o1}}, \boldsymbol{b_{o2}}, \boldsymbol{b_{o3}}$) is a coordinate system that follows the horizontal motion of $\{b\}$, i.e. the Euler angles of $\{b_o\}$ in $\{n\}$ are always $(0,0,\psi)^T$.

The coordinate systems $\{n\}$, $\{b\}$, $\{b_o\}$ and $\{t\}$ are all dextral orthogonal coordinate systems. They are shown in Fig.2.

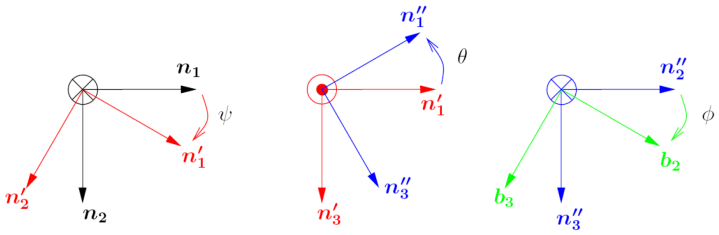

FIGURE 1. Euler angles and successive rotations from $\{n\}$ to $\{b\}$: ψ, θ, and ϕ are respectively the yaw, pitch and roll angles of the floating structure.

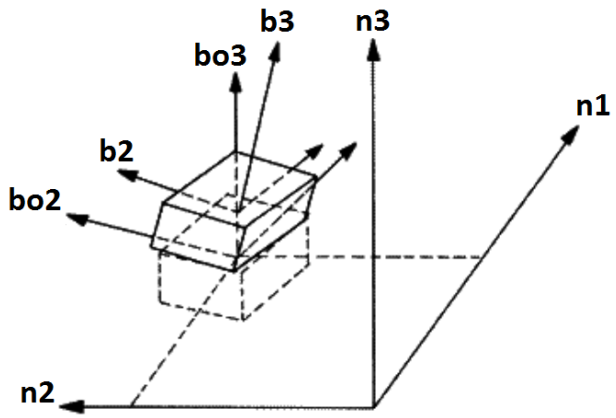

FIGURE 2. The different axes of the coordinate systems $\{n\}$, $\{b\}$ and $\{b_o\}$.

Hydrostatic pressure force on the hull

The purpose of this numerical model is to compute the hydrostatic pressure forces and moments on the hull for any position and attitude of the floater. We define the following quantities:

- ρ is the mass density of the water around the floating structure
- g is the acceleration of gravity
- Ω is the submerged volume
- B is the volume center of Ω
- $\boldsymbol{X_n}$ is a 3x1 matrix representing the coordinates of a point in $\{n\}$
- the quantities V_0 and $\boldsymbol{V_1}$ are defined by:

$$V_0 = \int_\Omega d\Omega \tag{1}$$

$$\boldsymbol{V_1} = \int_\Omega \boldsymbol{X_n} d\Omega \tag{2}$$

The hydrostatic pressure force on the hull is obtained by integrated the pressure gradient on the surface defining Ω. By using the Gauss theorem, we obtain the following expression for the buoyancy force $\boldsymbol{F}_{b_{\{n\}}}$ in $\{n\}$:

$$\boldsymbol{F}_{b_{\{n\}}} = \rho g \int_\Omega d\Omega \boldsymbol{n_3} = \rho g V_0 \boldsymbol{n_3} \tag{3}$$

The position of the application point B of the force $\boldsymbol{F}_{b_{\{n\}}}$ is given by:

$$\boldsymbol{OB}_{\{n\}} = \frac{\boldsymbol{V_1}}{V_0} \tag{4}$$

The moment in $\{b\}$ about O_b applied to the floating structure due to the hydrostatic force $\boldsymbol{F}_{b_{\{b\}}}$ is given by:

$$\boldsymbol{M}_{b_{\{b\}}} = \boldsymbol{O_b B}_{\{b\}} \times \boldsymbol{F}_{b_{\{b\}}} \tag{5}$$

Similarly to the method implemented in the program described in [7], the numerical model implemented in SIMO uses a hull geometry mesh based on N triangular panels. In practice, the STL (STereoLithography) file format is used as input. The meshed geometry needs to be watertight. Each panel is represented by three vertices with known position. Evaluating the contribution V_{0_i} of panel no. i to V_0 simply consists in computing the truncated prism volume contained between this panel and the water surface.

If a panel crosses the undisturbed water free surface, here the plane $\{z = 0\}$, only its submerged part contributes to V_0. A 'cutting procedure' illustrated in Fig. 3 is applied as follows:

- If all the three vertices of the panel are above the calm water plane, the panel is disregarded.

- If one vertex is above the calm water plane, the panel is cut at the calm water surface level. The intersection of the calm water surface with the edges of the panel defines two vertices, which are located on the calm water surface. Two new triangular panels are then defined based on the two vertices under the calm water surface and the two vertices on the calm water surface. They are included in the list of 'contributing panels'.

- If two vertices are above the calm water surface, the panel is cut at the calm water surface level. The intersection of the calm water surface with the edges of the panel defines two vertices which lay on the calm water surface. One new triangular panel is then defined based on the vertex under the calm water surface and the two vertices on the calm water surface. It is included in the list of 'contributing panels'.

- If all the three vertices are under the calm water surface, the panel is included in the list of 'contributing panels'.

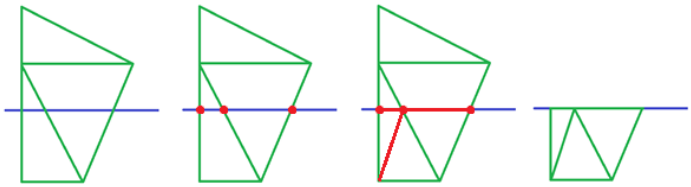

FIGURE 3. Different steps from left to right of the cutting procedure of panels next to the calm water surface. The hull mesh is in green. The blue line is the water surface. The red dots are the identified intersection points between the panel edges and the water surface. The red lines are the created panels edges. The last step on the far right of the figure shows the resulting "contributing" mesh used for the computation of the buoyancy force and moments.

With this cutting procedure, it is not necessary to refine the mesh about the calm water line. The mesh can be coarse as long as it describes the geometry correctly. All the vertices defined on the water surface are used to compute the area defined by the intersection of the body geometry with the water surface plane. This area is also known as the 'waterplane area'.

Since each panel is a triangle, an analytical solution can be used for V_{0_i} and V_{1_i}. The contributions of each panel are then summed up to compute the value of V_0 and V_1.

Weight of fluid in tanks

The purpose of this numerical model is to compute the hydrostatic forces and moments due to the mass of fluid contained in the N_c compartments of the floating unit. We assume that the free surface of the fluid in each compartment is always horizontal, i.e. parallel to the plan $\{\boldsymbol{n_1}, \boldsymbol{n_2}\}$. This ensures that the so called 'free surface effect' is included in the model. The calculation method is the same as the one described in the previous section, except that:

- The fluid contained in the compartment no. k has a mass density ρ_k which may be different from the water mass density ρ
- Since the fluid is *inside* the considered volume, the obtained force has an opposite sign: it corresponds to the weight of the fluid contained in the compartment
- The application point of the force is the center of gravity of the volume of fluid contained in the compartment

In addition, in order to compute the quantities V_0 and $\boldsymbol{V_1}$, the position of the fluid's free surface in the compartment needs to be determined, while it was known ($z = 0$) in the previous section. Indeed, for a given volume of fluid V_f contained in the compartment, the height of fluid h depends on the attitude of the compartment in $\{n\}$. The value of h is determined through an iterative secant method until a given volume accuracy is reached.

The possibility to model a damaged compartment has also been implemented. The model assumes that:

- The damaged compartment is completely open
- It is filled with the sea water surrounding the floating structure, i.e. ρ is used instead of ρ_k for the damaged compartment
- If the damaged compartment's geometry crosses the sea water surface, the position of the fluid's free surface level in the compartment is equal to the sea water surface level
- The damaged compartment is empty if it is located completely above the sea water level, and it is filled totally with sea water if completely submerged
- Physically, the result is exactly equivalent to subtracting the damaged compartment geometry from the hull when computing the buoyancy force

Wind and current forces on the floater hull

The wind and current forces and moments F_{wi} are computed based on dimensional coefficients C_i as follows:

$$F_{wi} = C_i(\gamma, z_b, \phi, \theta)V^2, \quad i \in [1,6] \tag{6}$$

where V is the fluid velocity (air or water) and γ its direction in the horizontal plane, relative to the $\boldsymbol{b}_{o1}$ axis. Here C_i depends

on the vertical position of the body z_b and its roll ϕ and pitch θ angles. The numerical model can thus capture variation of wind/current forces and moments due to large changes of draft and inclination angles of the floating structure. The coefficients C_i are interpolated linearly from a predetermined database.

This database contains in practice many datapoints, which makes experimental determination not realistic. However, wind tunnel tests can be used to validate some C_i coefficients of a database computed by Computational Fluid Dynamics (CFD) analyses, as specified in [8], section 5.8. An example of determination of wind and current loads on a semi-submersible by CFD along with a comparison with wind tunnel tests is presented in [9] and [10].

Equilibrium calculation

The goal of the equilibrium calculation is to find a position of the system where all the components of the resultant force $\boldsymbol{F_n}$ in $\{n\}$ (including moments) applied to the system are zero:

$$F_{ni} = 0, \quad i \in [1, N_d] \tag{7}$$

where N_d is the number of degrees of freedom of the system. If the system to be studied is a floating unit without horizontal stiffness (i.e. without anchor lines and without dynamic positioning system), the degrees of freedom to be included are typically the translation along $\boldsymbol{n_3}$ and the rotations about $\boldsymbol{n_1}$ and $\boldsymbol{n_2}$ ($N_d = 3$). If a horizontal stiffness is present, e.g. in the case of an anchored semi-submersible, all translations and rotations have to be included ($N_d = 6$).

We assume that the system has one unique equilibrium position and that this equilibrium is *stable*, i.e. it will return to this equilibrium position after any disturbance. The condition given by Eq.7 being difficult to fulfill numerically, a threshold (or error tolerance) $\boldsymbol{F_\varepsilon}$ is rather used. The values of all the components of $\boldsymbol{F_\varepsilon}$ are strictly positive. The condition that defines the equilibrium of the system is then given by:

$$\frac{1}{N_d} \sum_{i=1}^{N_d} \left(\frac{F_{ni}}{F_{\varepsilon i}}\right)^2 \leq 1 \tag{8}$$

The implemented calculation of the equilibrium is based on a Newton-Raphson method. The following iterative algorithm is used:

1. Assuming a position of the system, the resultant force in $\{n\}$ applied to the system is computed
2. The equilibrium criterion (Eq.8) is checked. If it is fulfilled, the equilibrium is found. If not, we proceed to step 3
3. The system stiffness in $\{n\}$ is computed locally by differentiation
4. A new position is computed based on the computed local stiffness and resultant force computed previously. We proceed to step 1

It is important to note that this equilibrium calculation has the following limitations:

- The calculation identifies one equilibrium position if it exists. However, if several equilibrium positions exists, only one will be found, and it may not be the one closest to the initial position.

- The identified equilibrium can be *unstable*, although Eq.8 is fulfilled. This may be resolved by introducing e.g. gradient descent methods.

Total restoring moment calculation

When studying the static stability of a floating unit, it is often practical to study the restoring moment of the floating unit about one specific axis. Relevant axes are typically 'weak' axes about which the stiffness is lower compared to other axes, e.g. the roll axis of a boat. Such specific axes are usually described by an *azimuth vector* $\boldsymbol{U_{a\{b_o\}}}$ included in the horizontal plane $\{\boldsymbol{b_{o1}}, \boldsymbol{b_{o2}}\}$ and with coordinates:

$$\boldsymbol{U_{a\{b_o\}}} = (x_a, y_a, 0)^T \tag{9}$$

The direction of $\boldsymbol{U_{a\{b_o\}}}$ defines the axis of rotation, known as the *azimuth axis*. The angle $\alpha = (\boldsymbol{b_{o1}}, \boldsymbol{U_{a\{b_o\}}})$ is known as the *azimuth angle*. The norm of the azimuth vector defines the positive rotation angle β of the body about the azimuth axis:

$$\beta = \|\boldsymbol{U_{a\{b_o\}}}\| = \sqrt{x_a^2 + y_a^2} \tag{10}$$

In practice, we extend the notation given in Eq.10: we use negative value of β for positive rotation about the opposite azimuth vector.

We assume that α and β are given. The goal of the implemented calculation is to compute the total restoring moment M_a about the azimuth axis for a rotation of angle β. In order to do so, the roll and pitch angles of the body are fixed to a value that corresponds to the rotation β about the azimuth axis. An equilibrium calculation is performed by including all degrees of freedom except the rotations about $\boldsymbol{n_1}$ and $\boldsymbol{n_2}$. For a case with hydrostatic forces only, this corresponds to the common fixed

trim approach described in e.g. [4]. The result is a position of the body where all forces and moments are zero, except the moments about $\boldsymbol{n_1}$ and $\boldsymbol{n_2}$. The resultant moment $\boldsymbol{M}_{b_o}$ is projected on the azimuth axis to obtain M_a.

In stability studies, the righting arm GZ is usually presented [11], the corresponding moments being computed about the center of gravity G and the considered forces only consisting of buoyancy and gravity. Herein, the notation GZ_t is introduced:

$$GZ_t(\beta) = -\frac{M_a(\beta)}{\rho g V_0(\beta)} \tag{11}$$

where V_0 is defined in Eq.1.

It is an extension of the common definition of GZ, in the sense that:

- It refers to the total moment applied to the body, including all type of forces such as wind and mooring line tension, and not only the buoyancy and gravity forces.
- The total moment is computed at the floater origin O_b, and not at the floater center of gravity.

This is also implicitly done in e.g. [5] where GZ quantities due to effects of mooring lines are presented.

Stability map calculation

The goal of the stability map is to get an overview of the static stability of the floating unit. The stability map presents the total restoring moment $\boldsymbol{M}_{b_o}$ for different rotation angles and rotation axes, similarly to the method presented in [3], based on a fixed trim and heel approach. All the equilibrium positions are identified, as well as their stability.

The goal of the implemented calculation is to compute the total restoring moment in $\{b_o\}$ as a function of the azimuth vector: $\boldsymbol{M}_{b_o}(\boldsymbol{x_a}, \boldsymbol{y_a}) = (M_1(x_a, y_a), M_2(x_a, y_a), 0)^T$. In order to do so, we define a grid of (x_a, y_a) values. For each point of the grid, a restoring moment calculation is performed as described in the previous section, except that the moment $\boldsymbol{M}_{b_o}$ is kept as such (and not projected on the azimuth vector).

The so-called 'stability map' is built based on the values of $\boldsymbol{M}_{b_o}$ as shown in Fig.7. The normalized values of $\boldsymbol{M}_{b_o}(x_a, y_a)$ are plotted as a vector field. The norm of $\boldsymbol{M}_{b_o}(x_a, y_a)$ is plotted in terms of contour plots in order to distinguish the areas with large and low restoring moments. Each intersection of the iso-contours $M_1 = 0$ and $M_2 = 0$ defines an equilibrium position for all degrees of freedom; indeed all the other force components are already zero since the equilibrium has been solved for the rotation about $\boldsymbol{n_3}$ and all the translations. The stability is assessed by linearizing $\boldsymbol{M}_{b_o}$ in the neighborhood of each equilibrium position $(x_{a_{eq}}, y_{a_{eq}})$ with the corresponding local gradient matrix. An equilibrium position is found stable if the linearized restoring moment is such that the floater tends to return to the equilibrium position for disturbances in any direction ζ in the (x_a, y_a) plane. In practice, the following procedure is applied:

- The gradient of the moment field is computed at the equilibrium position:
  $\boldsymbol{H}(x_{a_{eq}}, y_{a_{eq}}) = \begin{pmatrix} \frac{\partial M_1}{\partial x_a}(x_{a_{eq}}, y_{a_{eq}}) & \frac{\partial M_1}{\partial y_a}(x_{a_{eq}}, y_{a_{eq}}) \\ \frac{\partial M_2}{\partial x_a}(x_{a_{eq}}, y_{a_{eq}}) & \frac{\partial M_2}{\partial y_a}(x_{a_{eq}}, y_{a_{eq}}) \end{pmatrix}$
- For any point (x_a, y_a) in the neighborhood of the equilibrium position $(x_{a_{eq}}, y_{a_{eq}})$ the direction ζ is defined as:
  $x_a - x_{a_{eq}} = \cos\zeta$ and $y_a - y_{a_{eq}} = \sin\zeta$
- The change of moment in direction ζ is computed as $\Delta M(\zeta) = \boldsymbol{v}^{\boldsymbol{T}}(\zeta)\boldsymbol{H}\,\boldsymbol{v}(\zeta)$, where $\boldsymbol{v}(\zeta) = (\cos\zeta, \sin\zeta)^T$
- The maximum value of $\Delta M(\zeta)$ is found by solving the following equation:

$$\frac{\partial}{\partial \zeta}(\boldsymbol{v}^{\boldsymbol{T}}(\zeta)\boldsymbol{H}\,\boldsymbol{v}(\zeta)) = 0, \quad \zeta \in [0, 2\pi] \tag{12}$$

- If the obtained maximum change of moment is negative, the change of moment ΔM is then negative in all directions and the equilibrium is stable. Otherwise, it is unstable.

The quantity GM_t is defined from ΔM as an extension of the common GM:

$$GM_t(\zeta) = -\frac{\Delta M(\zeta)}{\rho g V_0} \tag{13}$$

where V_0 is defined in Eq.1.

SIMPLE TEST STUDIES

In order to validate the numerical model implemented in SIMO and described in the previous sections, some simple cases have been analyzed. The focus is on the precision of the hydrostatic force model, and the utility and limitations of the various types of calculations: equilibrium, restoring moment and stability map.

We consider a simple floater with the following characteristics:

- The hull of the floater is a cube with edge length $l = 10m$. It is modeled with a mesh of 12 triangular panels (2 on each face of the cube)
- The origin of the floater is the center of the cube
- The center of gravity of the floater is the center of the cube

- The coordinate system b is defined as in Fig.4
- The initial position and attitude of the floater are zero: $\boldsymbol{r} = \boldsymbol{0}$ and $\boldsymbol{\Theta} = \boldsymbol{0}$
- The mass density of the fluid surrounding the floater is $\rho = 1025 kg.m^{-3}$
- The mass of the floater is chosen to be $m = \frac{1}{2}\rho l^3 = 512500 kg$ so that the cube weight is equal to the buoyancy force at half length draft

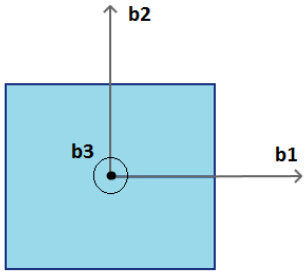

FIGURE 4. Coordinate system of the floater with cubic hull. Topview. Here, $\boldsymbol{\Theta} = \boldsymbol{0}$ so that $\boldsymbol{b}_{o_1} = \boldsymbol{b_1}$ and $\boldsymbol{b}_{o_2} = \boldsymbol{b_2}$

The floater is modeled in SIMO by using the implemented functionality described in the previous section. The forces acting on the floater are the weight and the buoyancy. By running an equilibrium calculation, i.e. by solving Eq.8, the equilibrium position found is indeed $\boldsymbol{r}_{eq} = \boldsymbol{0}$ and $\boldsymbol{\Theta}_{eq} = \boldsymbol{0}$. However, as mentioned previously, this result does not indicate if the equilibrium is stable or not; it is actually unstable as shown in the following. In order to have a better overview of the floater static stability, a restoring moment calculation is performed about the $\boldsymbol{b_{o2}}$ axis, corresponding to pure pitch rotations. In this case, $\alpha = 90 deg$, $\boldsymbol{b}_{o_2} = \boldsymbol{b_2}$ and $\beta = \theta$. The result is presented in Fig.5, together with the analytical solution. The following observations can be made:

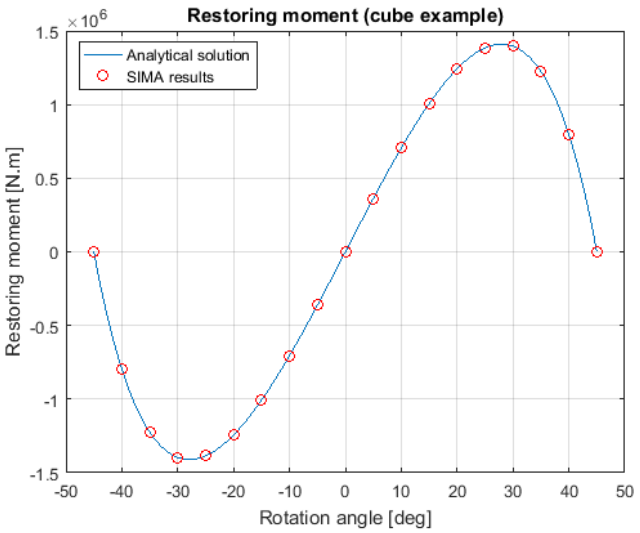

FIGURE 5. Restoring moment M_a as a function of the rotation angle β about the $\boldsymbol{b_{o2}}$ axis for the cube example. Red dots are the results from the SIMA computation. The blue line is the analytical solution.

1. The SIMA results match exactly the analytical solution. This is explained by the fact that the volume integration used for the computation of the buoyancy force uses an analytical formulation for each panel of the hull mesh. Since the hull geometry is exactly described by the mesh, the resulting volume integration of the whole mesh equals the analytical solution.
2. The restoring moment becomes zero for three values of rotation angle β: $-45 deg$, $0 deg$, and $45 deg$. Thus those three points are equilibrium positions. The equilibrium position found for $\beta = 0 deg$ concurs with the results from the simplified equilibrium calculation performed previously. This demonstrates that in some cases, a simple equilibrium position calculation is not enough to identify all the equilibrium positions.
3. The slope of the restoring moment is positive at the equilibrium $\beta = 0 deg$. This means that this equilibrium position is unstable about the $\boldsymbol{b_{o2}}$ axis.
4. The slope of the restoring moment is negative at the equilibrium positions $\beta = \pm 45 deg$. This means that the equilibrium positions are stable about the $\boldsymbol{b_{o2}}$ axis. However, there is no information about the stability of the equilibrium about the perpendicular axis. As shown in the following, those two equilibrium positions are actually unstable about the $\boldsymbol{b_{o1}}$ axis.

Observation no.1 does not apply in a case where a hull geometry cannot be described exactly by a triangular mesh. This is typically the case for geometries with curved lines and surfaces. For such geometries, increasing the number of panels generally increases the precision of the results. As an illustration, we consider a vertical cylinder of $10m$ height and $4m$ diameter. The floater is defined in an analogous manner as the cube example. A 'coarse' mesh of 176 panels is made, which divides each base circle into 30 segments. A 'fine' mesh is also used, with 1016 panels and dividing the base circles into 170 segments. The restoring moment about $\boldsymbol{b}_{o_2}$ is computed as for the cube example, using the two meshes. The differences with respect to the analytical solution are plotted in Fig.6. It can be observed that the fine mesh gives lower errors than the coarse one, illustrating the convergence of the implemented calculation.

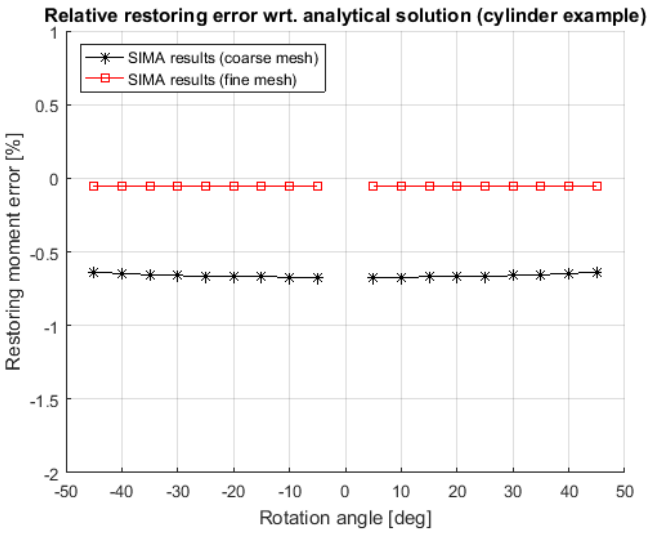

FIGURE 6. Resulting moment difference relative to the analytical solution for the cylinder example. The results from SIMA computations are shown as black stars (coarse mesh) and red squares (fine mesh). The points at $0deg$ inclination angle are not presented due to division by zero.

Observation no.4 demonstrates that a restoring moment curve (or the corresponding GZ_t curve) about one axis is not enough to conclude on the total stability of a floating unit. In order to get a complete overview of the system stability, we perform a stability map calculation using the cube example. The obtained stability map is shown is Fig.7. The restoring moment curve of Fig.5 corresponds to a cut of the stability map along the vertical line defined by $x_a = 0$. Along this line, we find again the three equilibrium positions identified in Fig.5. However, the gradient of M_1 is positive at those positions; thus they correspond to unstable equilibriums. This illustrates that a restoring moment (or GZ_t curve) calculation does not necessarily provide enough information on the complete stability of the system. This also demonstrates the utility of the stability map calculation: it provides a complete overview and a good understanding of the static stability of a floating unit.

REAL CASE EXAMPLES

In order to illustrate how the static stability calculations presented in the previous sections apply to real cases, a conventional semi-submersible production platform is considered. The main characteristics of the platform can be found in Table 1. A snapshot showing the platform modelled in SIMO is shown in Fig.8. Figure 9a) shows details of the hull and the coordinate system $\{b_o\}$. The hydrostatic model consists of the outer shell geometry including buoyant parts of the deck box, alongside all hull and deck box compartments, comprising its ballast tanks, voids and functional rooms. The tessellation from higher order geometry to the triangular mesh is carried out with low chord height and face normal deviations, yielding to a refined mesh when compared to the native geometry. The mesh of the platform hull is made of 77354 panels. Equilibrium positions are found with a precision of $F_\varepsilon = 10N$ for the forces and $F_\varepsilon = 100N.m$ for the moments. The calculation of the fluid volume in the compartments is performed with an accuracy of $0.001m^3$. Mooring lines and flexible risers are modelled by catenary lines, i.e. the physics of the lines is modelled by catenary equations in SIMO. We consider two different cases for which we assume no wave, no wind and no current.

Displacement	[Mg]	56 600
Draught	[m]	21
Field water depth	[m]	320
No. of mooring lines	[-]	4×4
Mooring pre-tension	[kN]	≈ 1470
No. of compartments	[-]	164
No. of flexible risers	[-]	19

TABLE 1. Main characteristics of the considered semi-submersible

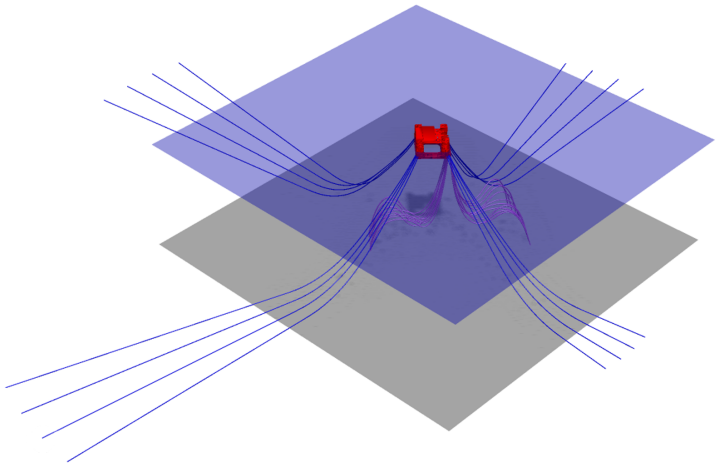

FIGURE 8. SIMO analysis model with the hydrostatic model indicated in red, mooring lines in blue and flexible risers in pink

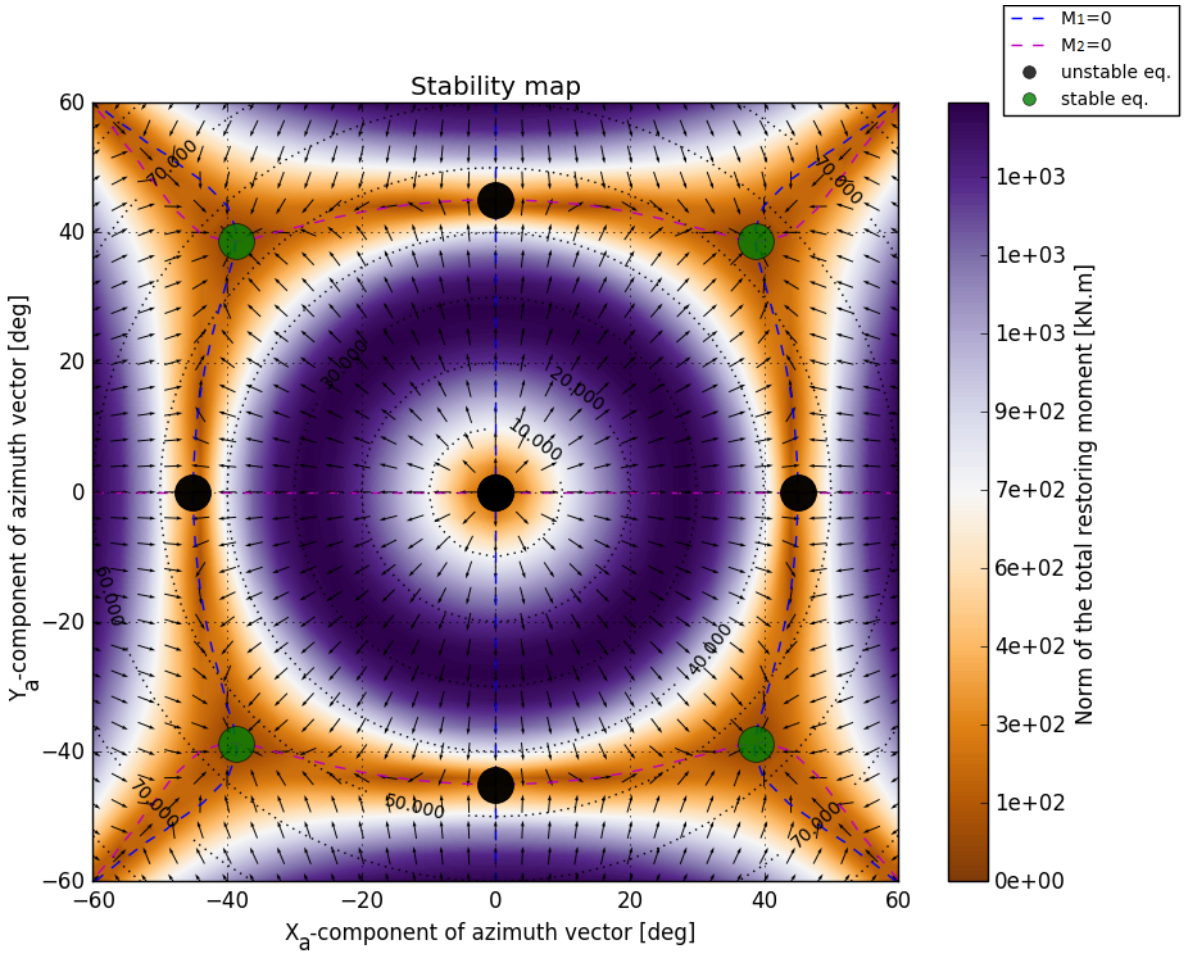

FIGURE 7. Stability map of the cube example. The horizontal and vertical axes of the plot are respectively the components x_a and y_a of the azimuth vector. The direction of the resulting moment $\boldsymbol{M}_{b_o}$ is indicated by the vector field, while its norm is represented by the colored field. Black dots indicates the unstable equilibrium positions while green dots indicates the stable ones. The blue and pink dashed lines represent the isolines of $M_1 = 0$ and $M_2 = 0$, respectively. The black dotted lines represent the isolines of the rotation angle β in degrees.

Case no.1: Flooded deck box

In a first real case example, the deck box bottom shown in Fig.12 has accidentally been flooded with sea water at 20% of its volume. It can be noted that this case is not a common case study, but is considered to be relevant and realistic for some designs. A simplified equilibrium calculation is performed. The obtained equilibrium position is presented in Fig.9, which is one solution out of potentially many. In order to assess the existence of other equilibrium positions, restoring moment calculations are performed about the longitudinal axis (azimuth angle $\alpha = 0deg$) and the transverse axis (azimuth angle $\alpha = 90deg$). The results are presented in Fig.10 in terms of GZ_t values (see eq.11). The two plots indicate four stable equilibrium positions (positive GZ_t slope) and one unstable position (negative GZ_t slope). For the same reasons discussed previously for the cube example (see observation no.4 in previous section), a stability map calculation is performed. The results are plotted in Fig. 11. In Fig.10, the GZ_t curves a) and b) correspond to a cut of the stability map along the axes $y_a = 0$ and $x_a = 0$, respectively. It can be observed that among the four equilibrium positions identified as stable by observation of the GZ_t curves, two of them are actually unstable: they are stable about one axis but unstable about the other one. The five equilibrium positions are presented in Table 2. The very low GM_t value of position no.1 is explained by the large vertical position of the deck box bottom as well as its large free surface effect; the fluid contained in the deck box bottom can freely move in the whole tank.

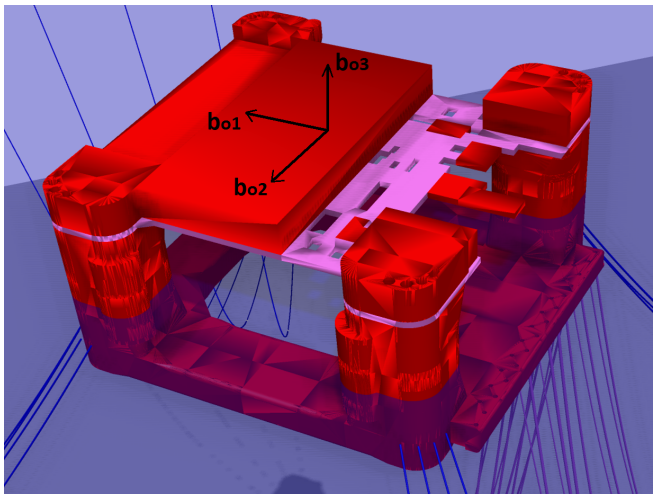

(a)

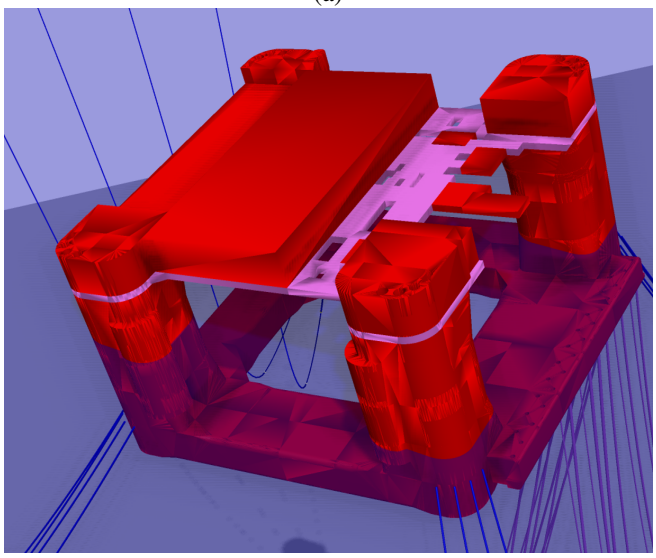

(b)

FIGURE 9. SIMO analysis model prior (a) and after (b) 20% flooding of the deck box bottom indicated in pink. In (a): upright with 21m draught. In (b): $\beta = 11.6deg$ heeling about azimuth $\alpha = 91.8deg$ with 22.1m draught. The inclination of the platform can be visualized by observing the water line at the platform columns in a) and b).

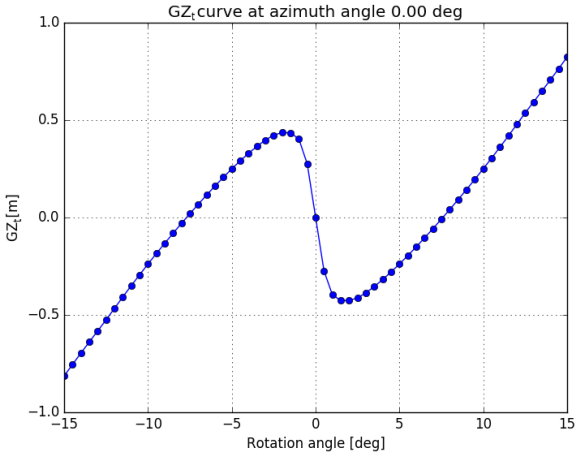

(a)

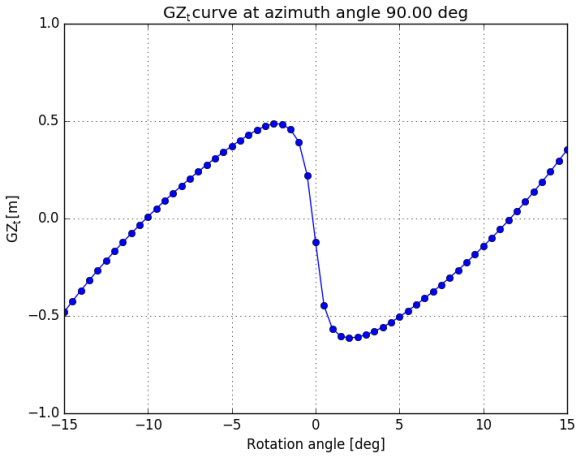

(b)

FIGURE 10. GZ_t curves of the considered platform for 20% flooding of the deck box bottom, corresponding to heeling about longitudinal axis $\alpha = 0deg$ (a) and transverse axis $\alpha = 90deg$ (b).

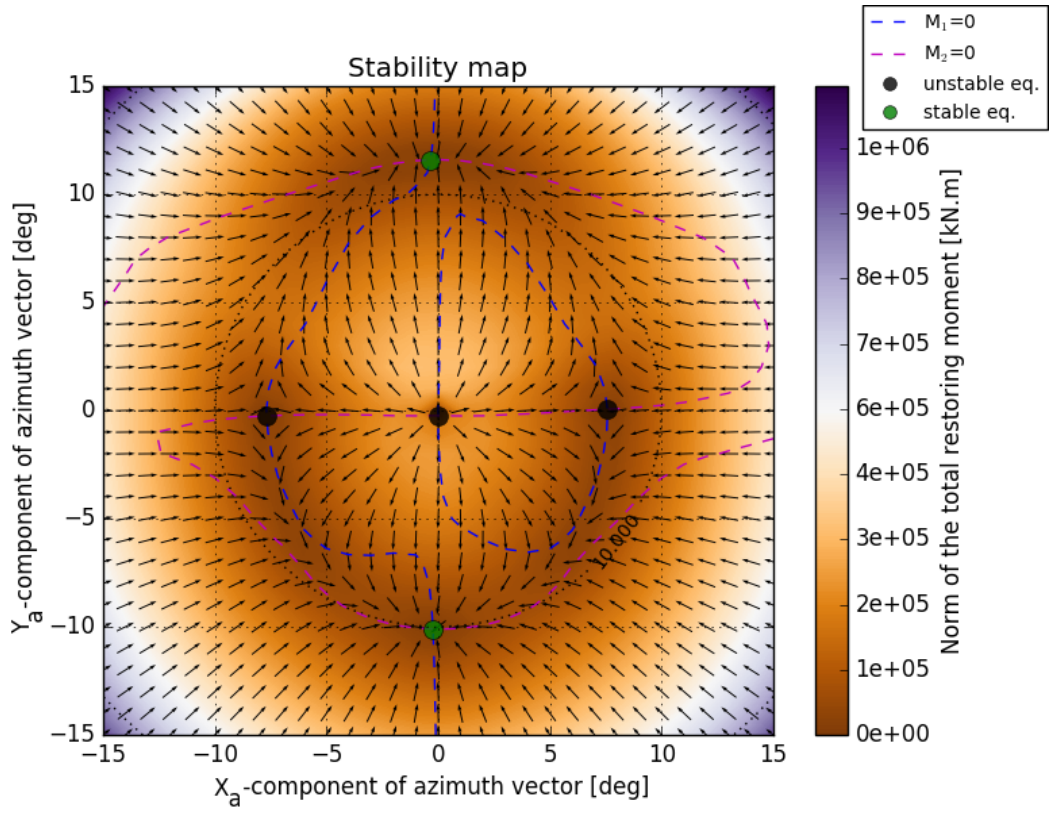

FIGURE 11. Stability map of the considered platform for 20% flooding of the deck box bottom. For further information regarding the nature of the plot, see caption of Fig.7

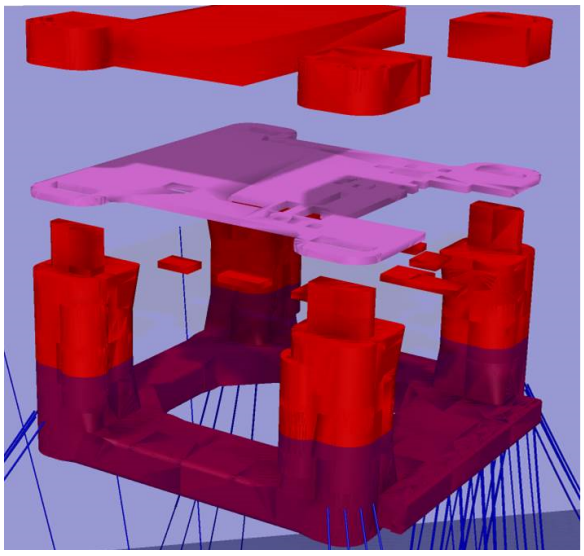

FIGURE 12. Exploded view of the SIMO analysis model. The deck box bottom in pink is one continuous tank.

Equilibrium Position no. [−]	Angle of rotation β [deg]	Azimuth angle α [deg]	Lowest GM_t value (see eq.13) [m]
1 (unstable)	-0.2	+90.5	-25.07
2 (unstable)	+7.6	+0.4	-3.81
3 (unstable)	-7.7	+1.9	-3.72
4 (stable)	-10.1	+88.7	+2.78
5 (stable)	+11.6	+91.8	+1.06

TABLE 2. Equilibrium positions of the considered platform for 20% flooding of the deck box bottom.

Case no.2: Damage recovery

In a second real case example, we consider a scenario where two non-adjacent void compartments have been damaged, due to e.g. a collision with a ship side. The damaged compartments are modeled in SIMO and equilibrium calculation is performed. The SIMO program is then used to define a damage recovery de-ballasting procedure. The goal of this procedure is to de-ballast compartments (i.e. reduce the quantity of ballast) in the neighborhood of the damaged compartments so that the platform recovers its initial attitude, i.e. upright with $21m$ draught. Figures 13a) and 13b) show the obtained equilibrium position of the platform, respectively before and after applying the de-ballasting procedure.

We now want to study the importance of the method used to model the anchor lines when assessing the stability of the platform after damage recovery. A second SIMO model is made by replacing the catenary anchor lines by fixed masses corresponding to the vertical tension of the lines for even keel with 21m draught. This procedure is commonly used to simplify anchor line systems in static stability analysis. The anchor lines then act as deadweights, without any stiffness. This SIMO model of the platform is thus regarded as 'freely floating' according to traditional stability analysis models. Stability map calculations are performed for the two SIMO models after damage recovery. Results are presented in Fig.14a) and Fig.14b) for the platform with anchor lines modeled as catenary lines and as deadweights, respectively. We can identify one stable equilibrium position for the model with catenary lines, which is the same as the one found previously (see Fig.13b)). Three equilibrium positions are identified for the model with deadweights: one unstable one and two stable ones. The equilibrium positions are listed in Table 3.

This shows that simplifying the modeling of the anchor lines system can clearly lead to a wrong picture of the system stability. It also shows that the stiffness of the positioning system has a large influence on the stability characteristics. This is particularly significant when considering damage recovery cases in which column compartments crossing the waterline suffer external damage, and where the hydrostatic stiffness is considerably reduced compared with the initial stiffness.

The damage recovery procedure applied in the analyzes was defined based on the model with catenary lines. If the damage recovery procedure were to be found by modeling anchor lines as deadweights only, a simple de-ballasting procedure would not have been sufficient: the unstability of the equilibrium position b.1 is not acceptable. In addition, it would have been necessary to increase the quantity of ballast in order to lower the vertical position of the platform center of gravity sufficiently to obtain positive stability restoring characteristics at even keel. The obtained procedure would have entailed two consequences:

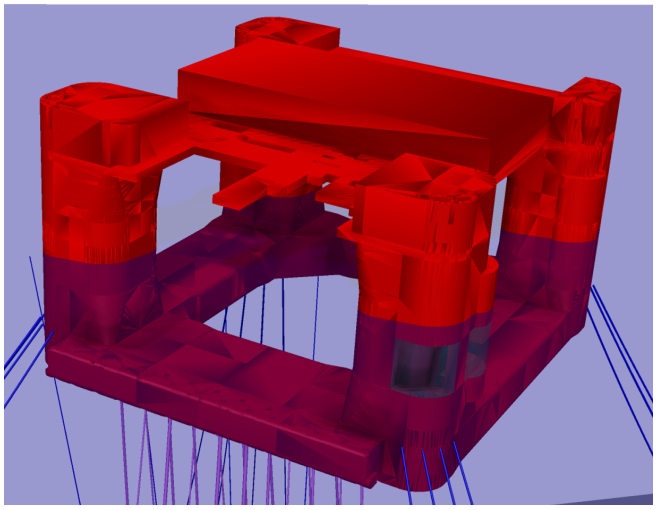

(a)

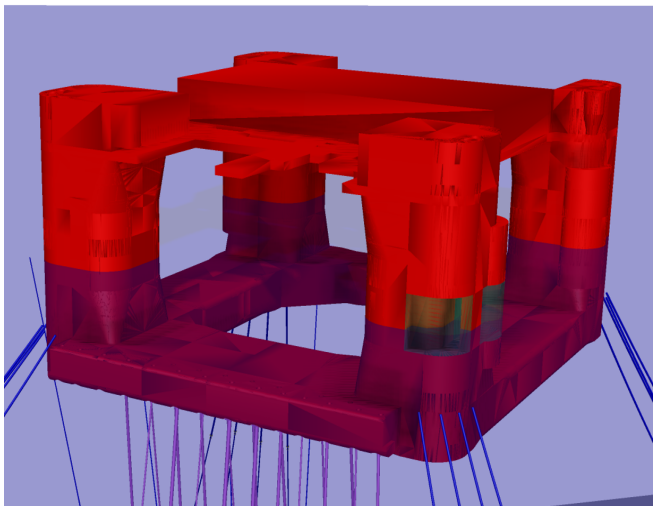

(b)

FIGURE 13. Equilibrium position of the SIMO analysis model prior(a) and after(b) damage recovery. The damaged compartments are shown in transparent green: they are completely submerged in (a) while they cross the sea water surface level in (b).

- When applying it, the personnel on board the platform would experience that the platform physical behavior is different from the behavior predicted by the analysis using anchor lines modeled as deadweights. This can make the personnel confused which is not desirable in emergency situations.
- It reduces the free board height and increases the hydrostatic pressure on watertight barriers on the compartments now exposed due the external damage.

The analysis of the actual stability of the system using the anchor

lines modeled as catenary lines shows that the damage recovery may be undertaken by a simple de-ballasting procedure and still maintains a stable unit at even keel. The latter is considered as a much safer operation. This stresses the importance of assessing all physical elements of importance in operational stability issues.

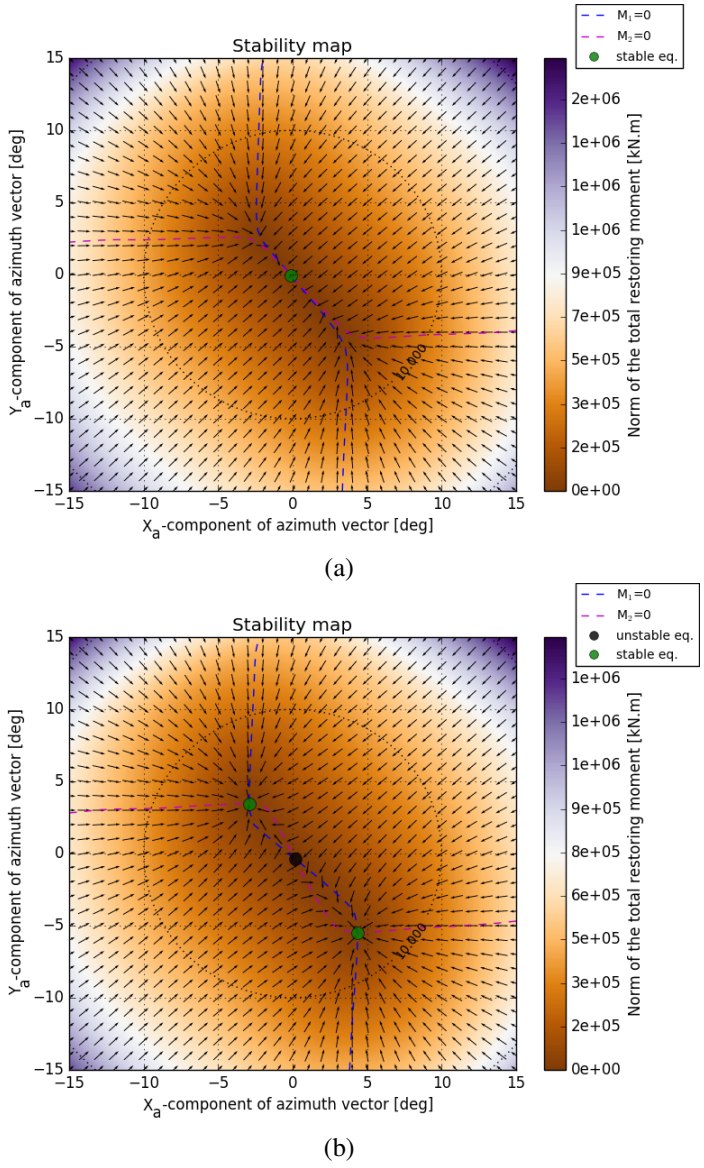

FIGURE 14. Stability map of the considered platform after applying the de-ballasting procedure for damage recovery. In (a): anchor lines are modeled as catenary lines. In (b): anchor lines are modeled as deadweights. For further information regarding the nature of the plot, see caption of Fig.7

Equilibrium Position no. $[-]$	Angle of rotation β $[deg]$	Azimuth angle α $[deg]$	Lowest GM_t value (see eq.13) $[m]$
a.1 (stable)	+0.1	-166.5	+0.13
b.1 (unstable)	+0.4	-67.3	-0.78
b.2 (stable)	-4.5	-49.9	+3.05
b.3 (stable)	+7.0	-51.5	+3.19

TABLE 3. Equilibrium positions of the considered platform after applying the de-ballasting procedure for damage recovery. Equilibrium position a.1 corresponds to the platform model with catenary lines. Equilibrium positions b.1, b.2 and b.3 correspond to the platform model with deadweights.

LIMITATIONS AND FURTHER WORK

The results presented in this paper corresponds to the work done so far. Although the relevance of the implemented tool has been illustrated through real case studies, further work is still needed in order to address the following points:

- The presented tool does not compute stability criteria as required in the rules and regulations. Such calculations should be implemented and the impact of using more realistic physical models should be investigated. In particular, it would be beneficial to implement equivalent acceptance criteria based on the stability map results, similarly to the studies presented in [3] or in [12].

- The concept of downflooding angle should be implemented in the presented tool.

- The effect of mean wave drift forces on the stability should be investigated. Such forces are responsible for an horizontal offset that modifies the mooring lines stiffness, whose impact on the platform's stability should be quantified.

- Sensitivity studies are necessary to quantify the necessary mesh properties required to achieve a given precision in the stability results. So far, calculations have been done with two meshes, one coarse and one fine, that lead to almost identical results.

- Additional implementation is necessary in order to include the dynamic effect of waves on the platform stability and quantify it. More generally, there is a need to investigate new methods to take into account dynamic effects in stability calculations. The presented tool being able to be run in time domain, it would be relevant and helpful for that purpose.

CONCLUSION

This paper illustrates that assessing the static stability of a floating unit in operational conditions requires precise and complete numerical tools capable of modeling accurately all the physical effects of importance. Numerical models for precise calculation of buoyancy on floater hull, weight of fluid in tanks and wind/current forces have been implemented in the SINTEF Ocean's software suite SIMA and validated against analytical solutions for simple geometries. The obtained numerical tool also benefits from all the verified and validated physical models present in SIMA, in particular the anchor line models. Real case examples presented in this paper show that studying static stability of a floating units requires to (1) consider static stability as a multidimensional problem (as e.g. the stability map proposed in this paper), and (2) include a complete and physical model of the mooring lines in the assessment of the static stability.

ACKNOWLEDGMENT

This work has been carried out as part of a project funded by STATOIL ASA.

REFERENCES

[1] Det Norske Veritas, 2014. Offshore Standard DNV-OS-C301, Stability and Watertight Integrity.

[2] IMO, 2009. Code for the construction and equipment of mobile offshore drilling units.

[3] Vassalos, D., Konstantopoulos, G., Kuo, C., and Welaya, Y., 1985. "A realistic approach to semisubmersible stability". *SNAME Transactions, Vol.93, pp. 95-128*.

[4] van Santen, J., 2013. "Problems met in stability calculations of offshore rigs and how to deal with them". *Proc. 13th International Ship Stability Workshop, Brest, September 2013*.

[5] Nishimoto, K., Brunozi, P. F., and Babadopulos, J. L., 1991. "Analysis of mooring lines and risers effects on the stability of semi-submersibles". *OMAE 1991, Volume I-B, Offshore Technology*.

[6] SINTEF, 2016. https://www.sintef.no/globalassets/project/oilandgas/pdf/simo.pdf.

[7] van Santen, J., 1986. "Stability calulations for jack-ups and semi submersibles". *International conference CADMO 1986*.

[8] Det Norske Veritas, 2014. Offshore Standard DNV-RP-C205, Environmental Conditions and Environmental Loads.

[9] Croonenborghs, E., Sauder, T., Fouques, S., and Reinholdtsen, S.-A., 2013. "Comparison of various methods for the assessment of wind and current loads on a semi-submersible platform". *Proc. Offshore Technology Conference, 2013*.

[10] Croonenborghs, E., Sauder, T., Fouques, S., and Reinholdtsen, S.-A., 2013. "CFD prediction of wind and current loads on a complex semi-submersible geometry". *Ship Technology Research, 60:3, 118-127*.

[11] Clauss, G., Lehmann, E., and Östergaard, C., 1992. *Offshore Structures volume 1: Conceptual Design and Hydrodynamics*. Springer-Verlag.

[12] Breuer, J. A., and Sjölund, K.-G., 2009. "Steepest descent method. resolving an old problem". *Proc. 10th International Conference on Stability of Ships and Ocean Vehicles, STAB2009, St. Petersburg*.